Channel Formation in Long Laser Pulse Interaction with a Helium Gas Jet

V. Malka, E. De Wispelaere, F. Amiranoff, S. Baton, R. Bonadio, C. Coulaud, and R. Haroutunian
Laboratoire pour l'Utilisation des Lasers Intenses, Centre National de la Recherche Scientifique, Ecole Polytechnique, 91128 Palaiseau Cedex, France

A. Modena
Imperial College, London, United Kingdom

D. Puissant and C. Stenz
Groupe de Recherches sur l'Energétique des Milieux Ionisés, Université d'Orléans, 45067 Orléans Cedex 2, France

S. Hüller
Centre de Physique Théorique, Centre National de la Recherche Scientifique, Ecole Polytechnique, 91128 Palaiseau Cedex, France

M. Casanova
Commissariat à l'Energie Atomique, Centre d'études de Limeil-Valenton, 94195 Villeneuve-St-Georges Cedex, France
(Received 22 April 1997)

Experimental realization of an electron density channel created by a low intensity laser in a helium gas jet is presented. The long (2.5 mm) plasma channel is fully ionized and thus prevents undesirable refraction effects for propagation and guiding of a subsequent high intensity laser pulse. The channel parameters are easily controlled and well suited for laser guiding. The radial plasma expansion and the temperature evolution have been measured and compared to hydrodynamic simulations which show that the plasma expansion is governed by a thermal wave during the laser pulse. [S0031-9007(97)04351-2]

PACS numbers: 52.40.Nk, 52.50.Jm

The propagation over a long distance of high intensity laser beams in a plasma is a crucial requirement for laser plasma acceleration schemes [1–3], x-ray lasers [4], high harmonic generation [5], and inertial confinement fusion [6]. All these schemes depend on the interaction length, which is typically limited by laser diffraction to a few times the Rayleigh length. Various mechanisms can help to overcome this limitation. Relativistic and ponderomotive self-channeling [7,8] is the natural way to do this, but it is not easy to obtain. Self-guiding in a preformed channel seems to be the most promising method to achieve propagation lengths of the order of ten times the Rayleigh length. Recent experiments have proven the feasibility of this idea. Durfee and Milchberg [9,10], have demonstrated the guiding of a low intensity laser pulse (10^{14} W/cm^2) in a nonfully ionized plasma channel created by focusing another laser pulse with an axicon in a gas-filled chamber. Clark and Milchberg [11] have recently characterized the evolution of this type of waveguide. In a recent experiment, Ehrlich *et al.* [12] demonstrated the guiding of an intense laser beam (10^{16} W/cm^2) focused into a slow capillary discharge over a distance of 11 times the Rayleigh length.

At high laser intensity and high plasma density the laser must propagate in vacuum before reaching the interaction zone to avoid refraction effects due to ionization [13]. In the case of a short (120 fs) and intense (10^{17} W/cm^2) laser pulse, it has recently been shown [14] that above a neutral density of 10^{18} cm^{-3} the focused laser intensity is reduced significantly (up to a factor of 10). The use of a helium gas jet represents a simple and elegant solution to get high intensity laser guiding without refraction due to ionization. It is important that the laser propagates in vacuum or in a fully ionized plasma before reaching the focal zone. By focusing the laser beam on the sharp edge of the gas jet and by using helium which is easily fully ionized, we can be sure that the pulse to be guided does not propagate in any nonfully ionized plasma. In this Letter we present the first detailed demonstration of channel formation in the interaction of a 600 picosecond laser beam with a helium gas jet. Our experimental results show that a long electron-depleted fully ionized channel is formed along the whole length (2.5 mm) of the gas jet by hydrodynamic radial expansion due to collisional heating. Various diagnostics are used to measure the evolution of the channel. The evolution of electron temperature and density are deduced from time resolved Thomson scattering. Radial hydrodynamic expansion is measured by time resolved Schlieren imaging, and the electron depletion is deduced from interferometry. Comparison with a one-dimensional (1D) hydrodynamic code shows very good agreement with all of the experimental data.

The experiment was performed at the Laboratoire pour l'Utilisation des Lasers Intenses (LULI). The infrared ($\lambda_L = 1.053$ μm) neodymium-glass laser beam is frequency doubled using a KDP crystal giving a maximum energy of 25 J at 0.526 μm. The laser is linearly polarized at 45° compared to the horizontal plane. The pulse duration of the frequency-doubled pulse is 600 ps full width

at half maximum (FWHM) with a Gaussian shape. The 90 mm diameter laser beam is focused on the edge of a helium gas jet with an $f/3$ doublet lens to a 28 μm FWHM diameter focal spot which is seven times the diffraction limit of a perfect Gaussian beam. The average laser intensity in vacuum is about 5×10^{15} W/cm^2. The Rayleigh length calculated by geometric optics (considering the half width at half maximum of the laser intensity) is in rough agreement with the experimental one, which is measured to be about 250 μm. To obtain interferograms and Schlieren images, a 600 ps collimated probe beam at 0.526 μm propagates through the plasma at 90° from the interaction beam. Schlieren images of the radial evolution at focus are measured by a streak camera with a 25 ps time resolution. To obtain the evolution of the plasma parameters (electron density and electron temperature), self-emitted Thomson scattering is collected with an $f/2.5$ achromatic lens at 45° from the incident laser beam on the horizontal plane (i.e., at 60° from the laser polarization axis) and resolved both temporally and spectrally by a spectrometer-streak camera system. The slit of the streak camera limits the source radial size to 50 μm.

The main results we present in this Letter concern the hydrodynamic evolution of the plasma. Figure 1 shows the time integrated interferograms of the plasma. The images are recorded 530 ps after the interaction beam (i.e., the delay between the peaks of the interaction and probe beam is 530 ps). At this time, the plasma expansion is in a quasistationary regime and the 600 ps time integrated interferometer shows well-defined fringes. Figure 1(a) corresponds to a high laser intensity case (5×10^{15} W/cm^2). The radial plasma size is about 300 μm diameter, and the plasma covers the whole length (2.5 mm) of the gas jet. Figure 1(b) corresponds to a lower laser intensity case (7×10^{14} W/cm^2) and shows a slightly shorter (1.8 mm) and narrower plasma (with 200 μm diameter). Assuming cylindrical symmetry, we can deduce the radial electron density profile via Abel inversion. The result is plotted in Fig. 2 for the position marked by the arrow in Fig. 1. In both cases, these profiles show a strong density depletion on the laser axis. For example, in the lower intensity case, the density varies from a value of 2×10^{19} cm^{-3} on the laser axis to a peak of 7×10^{19} cm^{-3} at a radial position of 100 μm. Although the Abel inversion is not capable of determining the exact central value with high accuracy, the measurements using Thomson scattering confirmed these values.

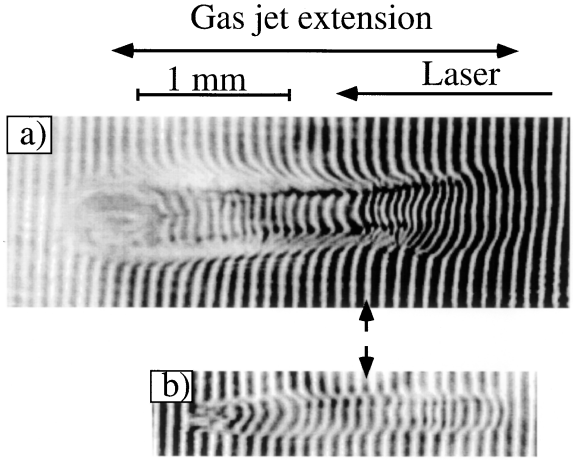

FIG. 1. Time integrated interferograms at two laser intensities: (a) $I_L = 5 \times 10^{15}$ W/cm^2 and (b) 7×10^{14} W/cm^2.

We also determine the evolution of the electron density and temperature by time resolved Thomson scattering of the interaction beam. Light is collected at 45° from the laser axis from various positions along the axis and shows a similar behavior along the whole gas jet, in agreement with the interferograms. Time resolved Thomson scattering spectra at a gas jet pressure of 1.4 bar are presented in Fig. 3(a). The electron satellites are clearly visible on both sides of the ion peak and are separated by the Bohm-Gross frequency $\omega = (\omega_p^2 + 3k^2 v_t^2)^{1/2}$, where $\omega_p = (4\pi n_e e^2/m)^{1/2}$ is the electron plasma frequency, k is the electron plasma wave number, and v_t is the electron thermal velocity. In order to measure both ion and electron features on a single shot, the ion peak is attenuated by a factor of 100. The time evolution of the electron satellites shows a quick (less than 100 ps) and complete ionization of the gas in the focal region very early in the pulse frame. We then observe convergence of the red and blue electron satellites as a function of time, which clearly indicates a strong decrease of the electron density on the laser axis. The variation of the electron density with time is shown in Fig. 3(b), where it decreases from 7×10^{19} to 2×10^{19} cm^{-3} during the interaction time. The electron density profiles deduced from both the interferograms and the Thomson scattering measurements clearly indicate that the conditions needed to guide a subsequent (second) laser pulse are satisfied [9,10].

In order to get more insight into the hydrodynamic evolution of the plasma due to the absorbed laser energy along the laser axis, we performed simulations with the one-dimensional hydro code MULTI [15]. This code solves the hydrodynamic equations in Lagrangian coordinates, it includes electron heat transport, and uses tabulated

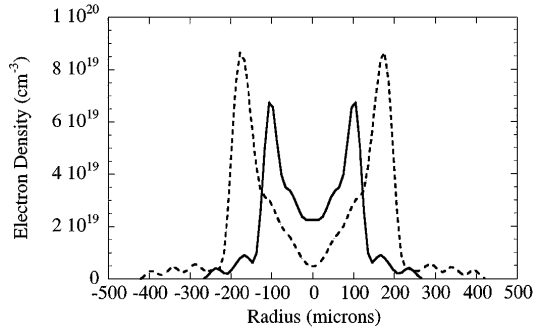

FIG. 2. Electron density profile for the positions marked by the arrow in Figs. 1(a) (dotted line) and 1(b) (solid line).

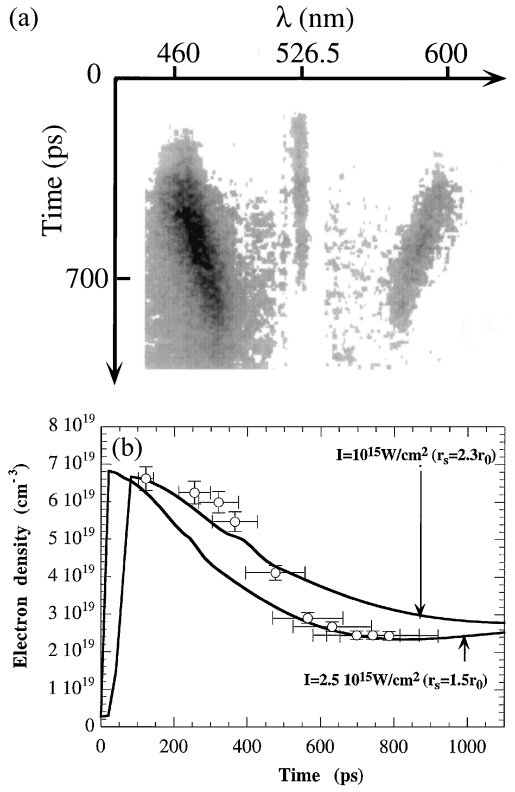

FIG. 3. (a) Time resolved Thomson scattering spectra at 45° to the laser axis. The ion peak is attenuated by a factor of 100. (b) Electron density deduced from (a) by the Bohm-Gross relation taking into account the thermal correction (dots), and simulation results at two different laser intensities (solid line) with the same power (38 GW). r_0 and r_s are, respectively, the vacuum radius and the estimated radius in the plasma.

equation-of-state data. It also includes multigroup radiation transport which is of minor importance in the present context. The version of the code used here solves the equations in cylindrical geometry. The cylinder axis corresponds to the laser propagation axis. The code was modified such that the laser energy deposition is localized in a specific volume around the cylinder axis. Except for an early stage of the interaction when the helium gas undergoes field or tunnel ionization in a small radius around the laser axis where the laser field is maximum, ionization is dominated by collisions. In the simulations, we assume that the plasma is completely preionized within a radius of the size of the laser spot, and we use tabulated data for the subsequent ionization of the outer gas (obtained from the code SNOP [16]). In order to model the ponderomotive contribution to the formation of the channel, we include a ponderomotive term in the equation of motion of the fluid, assuming a Gaussian laser profile in the radial dimension. However, with our experimental parameters, ponderomotive effects do not modify the evolution significantly.

The evolution of the on-axis electron density is compared with simulation data in Fig. 3(b). In addition to the experimental data points, we show two curves from simulations assuming a Gaussian shape in time with a duration of 600 ps at FWHM and with a power (pulse energy) of $P_L = 38$ GW ($E_L = 25$ J). The simulations agree with the observed density depletion when we assume that the laser power is concentrated within a radius r_s between $1.5r_0$ and $2.3r_0$, where r_0 is the radius of the spot measured in vacuum. This apparent increase in spot size originates from small refraction effects induced by the ionization process. The discrepancy in the temporal behavior may be attributed to the simplified description of the pulse shape and the constant radial laser profile used in the code. Refraction stays considerably lower than in a gas-filled chamber case [17]; in this case, the corresponding time resolved Thomson spectra show that the electron density is constant in time without any sign of channel formation. This indicates that, in the gas-filled chamber case, refraction considerably reduces the maximum laser intensity reached at focus, and thus limits the plasma depletion.

From the Thomson scattering spectra we also extract the electron temperature evolution from the ratio between the ion and electron satellites [18]. The deduced electron temperature evolution is shown in Fig. 4. It follows the laser pulse shape, reaching a peak temperature of 250 eV. (A similar evolution has been measured by other diagnostics such as ion Thomson scattering.) In the same plot we also show the electron temperature deduced from the simulations (the focal spot radius in the simulation is $r_s = 1.5r_0$ but the temperature evolution does not vary significantly, taking either $r_s = 1.5r_0$ or $r_s = 2.3r_0$). The simulations clearly demonstrate that, from the beginning, the plasma is gradually heated by the absorbed light, generating an electron heat wave propagating into the plasma surrounding the laser-heated cylinder. This qualitatively reflects what is expected from self-similar solutions in laser-heated plasmas [19,20]. In contrast to recent experiments where a

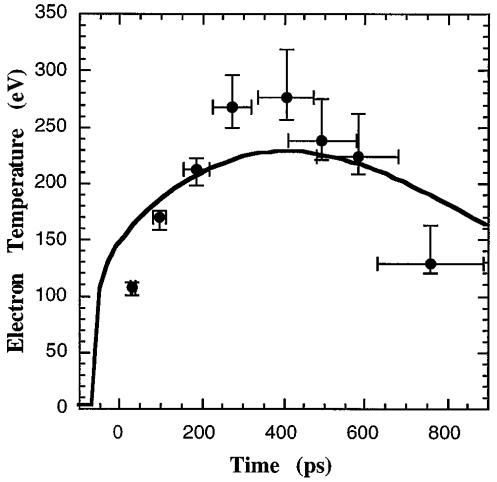

FIG. 4. Electron temperature evolution deduced from the time resolved Thomson spectra (dots) and simulation results (solid line).

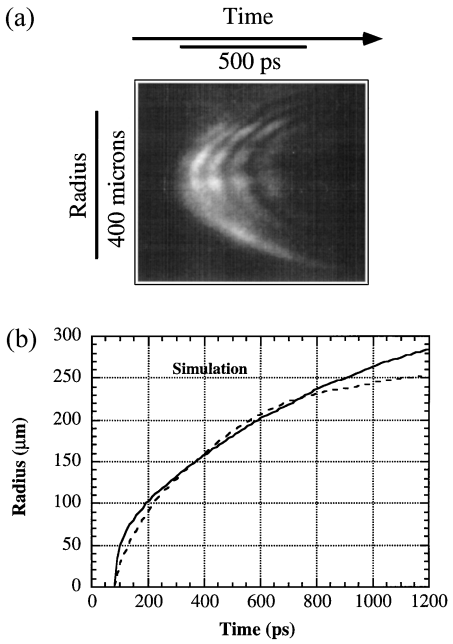

FIG. 5. (a) Time resolved Schlieren images. (b) Time resolved gas-plasma interface radius (dotted line) and simulation results (solid line).

shock wave drives the hydrodynamic expansion [11], the laser intensity in our experiments is high enough that heating due to collisional absorption drives a highly supersonic heat wave very early in the laser pulse. The formation of a shock front, however, is delayed until the speed of the heat wave drops to a value below the sound speed, which happens in our case at the end of the laser pulse. Behind this heat-wave front, the helium gas is ionized and heated up to the temperature observed experimentally, i.e., higher than 200 eV. The pressure gradient due to the temperature and electron density gradients gradually accelerates the plasma that starts expanding from the center and preferentially concentrates near the front of the heat wave. The interface, separating the cold gas from the heated plasma, can be observed as a gradient in the electron density. The Schlieren diagnostic is sensitive to electron density gradients and was used to determine the radial evolution of the channel. In Fig. 5(a) we show the time resolved Schlieren image at the focal position. The radial evolution of the gas-plasma interface is shown in Fig. 5(b) and is compared with MULTI simulations. These simulation results prove to be in good agreement with all of the experimental data.

In conclusion, we have studied the plasma channel evolution during the interaction of a 600 ps laser beam with a helium gas jet. Interferometry measurements show a deep channel in a fully ionized plasma produced even at relatively low laser intensities. The electron density channels that we observe easily satisfy the optical guiding condition for a realistic laser pulse without suffering from refraction effects. The Thomson scattering diagnostic shows a strong and rapid decrease of the electron density. The radial expansion of the plasma-gas interface is also measured. Simulations indicate that the generation of the electron density channel is a consequence of the expansion due to an electron heat wave. The channel parameters can be optimized by changing independently the laser intensity (energy, spot size, or pulse duration) or the gas pressure. Our results are of great importance where high-intensity optical guiding is needed.

The authors would like to acknowledge the support of the laser team of LULI. We would like to thank K. Eidmann for the tabulated ionization data which were used in the MULTI simulations.

[1] T. Tajima and J. Dawson, Phys. Rev. Lett. **43**, 267 (1979).
[2] A. Modena *et al.*, Nature (London) **377**, 606–608 (1995).
[3] E. Esarey, P. Sprangle, J. Krall, and A. Ting, IEEE Trans. Plasma Sci. **24**, 252–288 (1996).
[4] P. B. Corkum, N. H. Burnett, and F. Brunel, Phys. Rev. Lett. **62**, 1259 (1989).
[5] X. F. Li *et al.*, Phys. Rev. A **39**, 5751 (1989).
[6] M. Tabak *et al.*, Phys. Plasmas **1**, 1626 (1994).
[7] A. B. Borisov *et al.*, J. Opt. Soc. Am. B **11**, 1941 (1994).
[8] A. B. Borisov *et al.*, Phys. Rev. A **45**, 5830 (1992).
[9] C. G. Durfee III and H. M. Milchberg, Phys. Rev. Lett. **71**, 2409 (1993).
[10] C. G. Durfee III, J. Lynch, and H. M. Milchberg, Phys. Rev. E **51**, 2358 (1995).
[11] T. R. Clark and H. M. Milchberg, Phys. Rev. Lett. **78**, 2373–2376 (1997).
[12] Y. Ehrlich *et al.*, Phys. Rev. Lett. **77**, 4186 (1996).
[13] P. Monot *et al.*, J. Opt. Soc. Am. B **9**, 1579 (1992).
[14] V. Malka *et al.*, Phys. Plasmas **3**, 1682–1688 (1996).
[15] R. Ramis, R. Schmalz, and J. Meyer-Ter-Vehn, Comput. Phys. Commun. **49**, 475 (1988).
[16] K. Eidmann, Laser Part. Beams **12**, 223 (1994).
[17] E. DeWispelaere *et al.*, (to be published).
[18] J. Sheffield, *Plasma Scattering of Electromagnetic Radiation* (Academic, New York, 1975).
[19] S. I. Anisimov, JETP Lett. **12**, 287 (1970).
[20] Y. B. Zeldovich and Y. P. Raizer, *Physics of Shock Waves and High-Temperature Hydrodynamic Phenomena* (Academic, New York, 1967).